

The Polynomial Spiral and Beyond

Cye H. Waldman

cye@att.net

Copyright 2013

Introduction

The term polynomial spiral was coined by Dillen (1990). It is a generalization of the spiral of Cornu, aka Euler's spiral, and defined parametrically in terms of the arc length as follows

$$z(s) = \int e^{iP_k(s)} ds \quad (1)$$

where $P_k(s)$ is a k^{th} -order polynomial. The distinguishing feature of the polynomial spiral is that the curvature is given simply by $\kappa(s) = P'_k(s)$, i.e., the derivative of P_k , a polynomial of order $k-1$. This can be readily derived from the equation for the curvature of a plane curve in the complex plane given by Zwikker (1963),

$$\kappa(s) = \frac{1}{\rho(s)} = \frac{\mathcal{Im}\{z' \cdot z''\}}{|z'|^3} = \mathcal{Im}\left\{\frac{z''}{z'}\right\} \quad (2)$$

where the last equality follows from the fact that $|z'(s)| = 1$. This is perhaps not a well-known property of the natural form of spirals (i.e., those expressed in terms of the arc length). It follows from the equation for the arc length of a complex curve in terms of an arbitrary parameter, to wit,

$$s = \int |z'(u)| du \quad (3)$$

The polynomial spiral is mostly known for its fanciful spirals, first shown in Dillen's paper. They are reproduced here in Figure 1 and Figure 2, along with some of our own creation with random coefficients in 5th and 6th-order polynomials (Figure 2, lower panels). The attached animations are derived from the figures in the lower panels of Figure 1 and Figure 2.

The higher the order of the polynomial, the more complex are the curves (i.e., more inflection points). Figure 3 shows the results for a 10th-order Euler polynomial. Figure 4 shows the same curve (blue) stretched out normal to the complex plane (yellow), along with its real (red) and imaginary (green) parts.

This brief note outlines a generalization of the polynomial spiral and an alternative form that is expressed in terms of the tangent angle instead of the arc length. This is followed by a demonstration of the principle for log-aesthetic curves and the derivation of analytic and closed-form solutions thereof. Finally, we introduce a new class of polynomial spirals, for which the radius of curvature is a polynomial in terms of the tangent angle and derive analytic solutions.

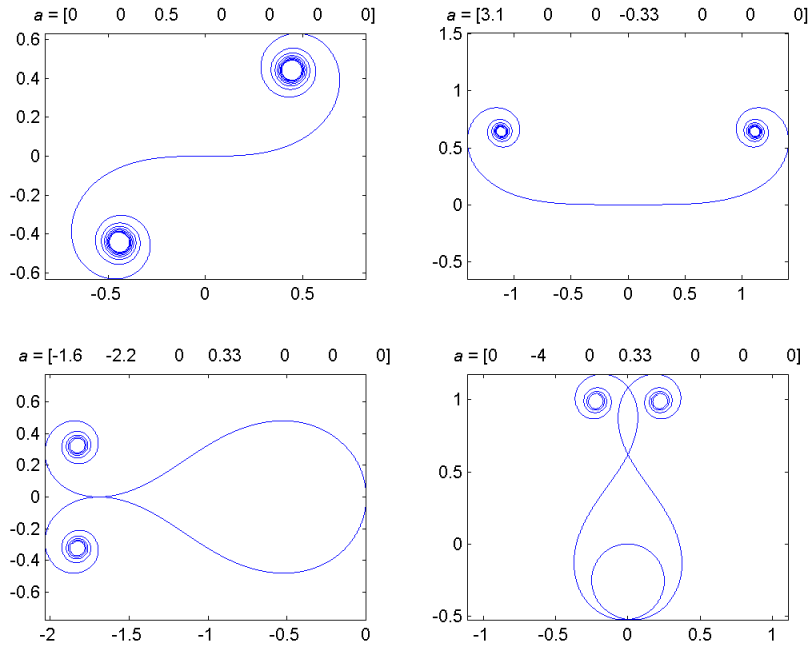


Figure 1: Examples of polynomial spiral curves: $P_k(s) = \sum_{k=0}^6 a_k s^k$.

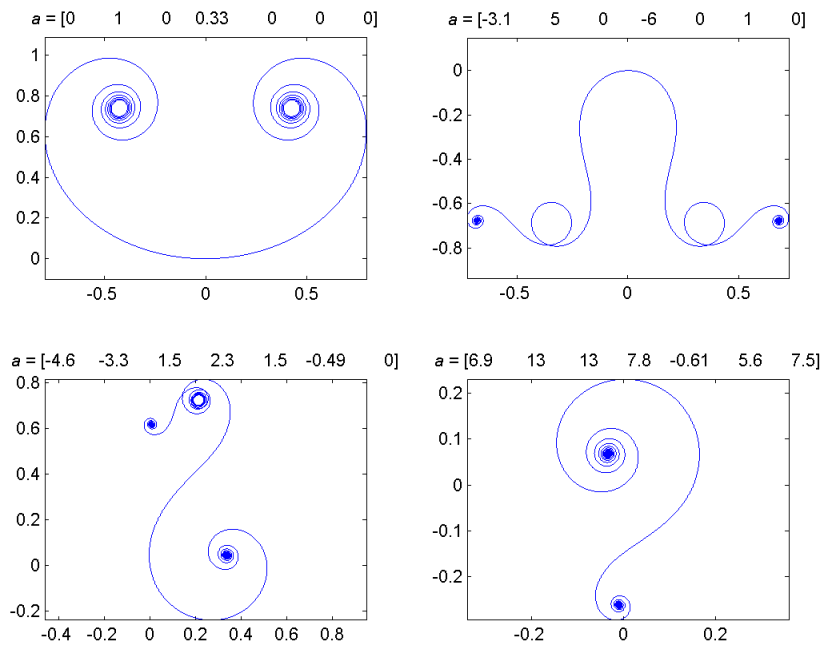


Figure 2: More examples of polynomial spiral curves: $P_k(s) = \sum_{k=0}^6 a_k s^k$.

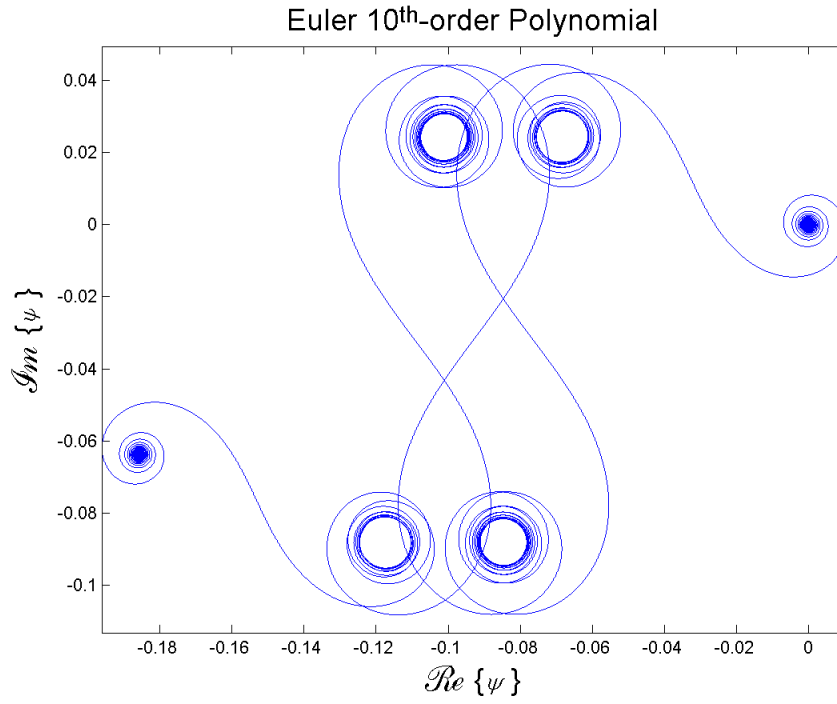


Figure 3: Euler 10th-order Polynomial.

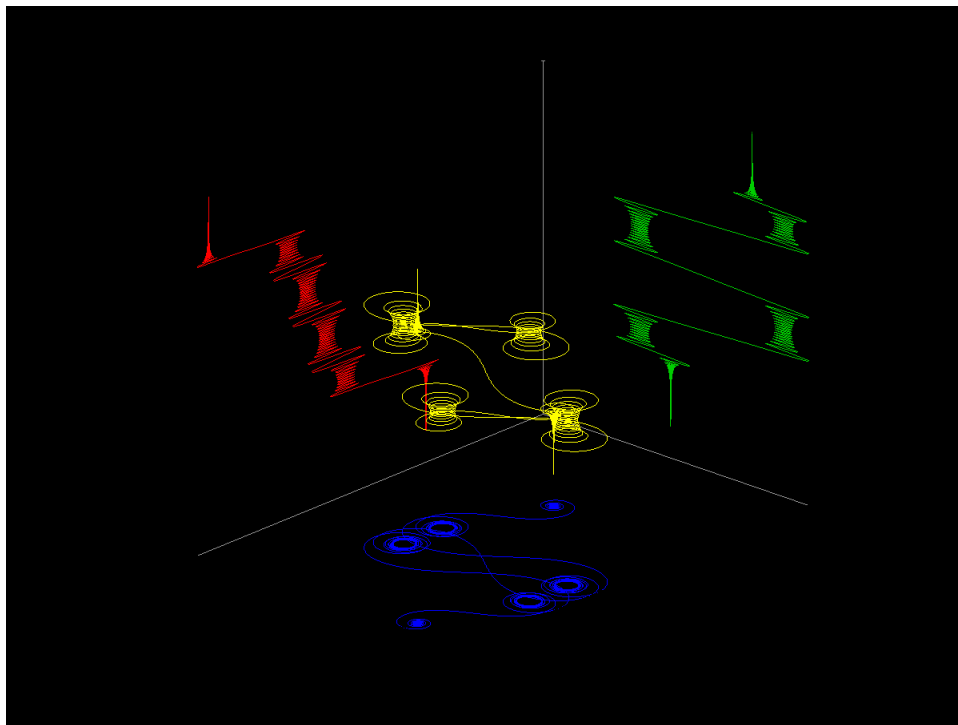


Figure 4: Euler 10th-order Polynomial, 3-D rendition.

Generalization

There is nothing intrinsic to Eqs. (1) or (2) that limit them to polynomials. It is therefore apparent that **all** curves can be expressed parametrically in terms of the arc length as follows:

$$z(s) = \int e^{i \int \kappa(s) ds} ds = \int e^{i\theta(s)} ds \quad (4)$$

$$\frac{d\theta}{ds} = \kappa(s)$$

where θ is the tangent angle. Moreover, invoking the above, we may transform the variables from arc length to tangent angle as follows

$$z(\theta) = \int \frac{e^{i\theta}}{\kappa(\theta)} d\theta = \int \rho(\theta) e^{i\theta} d\theta \quad (5)$$

where $\rho = 1/\kappa$ is the radius of curvature.

We *cannot*, however, transform to an arbitrary parameter, say u , because we end up with an integral equation, viz.,

$$z(u) = \int |z'(u)| e^{i\theta(u)} du \quad (6)$$

$$\frac{ds}{du} = |z'(u)|$$

Application to log-aesthetic curves

In many areas of industrial design, computer-aided geometric design, and typography, designers are charged with the task of fitting a “fair” curve to a set of points. To quote Burchard *et al.*, (1994): ‘ “Fairness” in this sense means that the curve must not only be “smooth” in a mathematical sense, but that it must be pleasing to the eye. In other words, there are *aesthetic* considerations that constrain the curve fitting operation.’ One such class of curves is the log-aesthetic curves. These are based on the notion that some aesthetic curves have the property of logarithmic curvature histograms. The spiral of Cornu and the logarithmic spiral are examples of such. These curves are discussed in detail by Yoshida and Saito (2006) and Ziatdinov *et al.* (2012). The purpose of this section is multi-fold. First, we will develop the equations for the log-aesthetic curves in terms of the generalized polynomial spiral, i.e., Eqs. (4) and (5). Second, we will derive analytic solutions for these equations in terms of the incomplete gamma function, as suggested by Ziatdinov *et al.* The present solutions are compact and tractable. And finally, we will demonstrate closed-form solutions for a specific class of incomplete gamma functions. We will confine our attention to the non-trivial cases; these will be denoted by the exclusion of certain values of the slope α .

The fundamentals of log-aesthetic curves are adequately described in the above-mentioned references and will not be repeated. They begin with the definition of log-aesthetic curves as

$$\log\left(\rho \frac{ds}{d\rho}\right) = \alpha \log \rho + c \quad (7)$$

$$\frac{ds}{d\rho} = \frac{\rho^{\alpha-1}}{\lambda}$$

where the constant $c = -\log \lambda$ is the point of intersection with the y-axis and α is the slope.

We will use the following equivalent equations as the point of departure for the present analysis:

$$\frac{d\kappa^{-\alpha}}{ds} = \lambda\alpha$$

$$\kappa^{-\alpha} = \lambda\alpha s + c \quad (\alpha \neq 1) \quad (8)$$

$$\kappa(s) = (\lambda\alpha s + 1)^{-1/\alpha}$$

where $\kappa = 1/\rho$ is the curvature and we have chosen the constant such that $\kappa(0) = 1$. We can determine the tangent angle from the curvature as follows

$$\theta(s) = \int \kappa(s) ds = \frac{(\lambda\alpha s + 1)^{\frac{1}{a}}}{\lambda(\alpha - 1)} + c \quad (9)$$

$$= \frac{(\lambda\alpha s + 1)^{\frac{1}{a}} - 1}{\lambda(\alpha - 1)} \quad (\alpha \neq 0, 1)$$

where $a = \alpha/\alpha - 1$ and we have chosen the constant such that $\theta(0) = 0$.

Finally, we can determine $\kappa(\theta)$ as required for Eq. (5) by solving Eq. (9) for $s(\theta)$ and substituting in Eq. (8) to obtain

$$\kappa(\theta) = [\lambda(\alpha - 1)\theta + 1]^{\frac{1}{\alpha-1}} \quad (10)$$

The solutions for the log-aesthetic curves can now be expressed in terms of the arc length or tangent angle as follows:

$$z(s) = \int e^{i \frac{(\lambda\alpha s + 1)^{\frac{1}{a}-1}}{\lambda(\alpha-1)}} ds \quad (11)$$

$$z(\theta) = \int [\lambda(\alpha - 1)\theta + 1]^{\frac{1}{\alpha-1}} e^{i\theta} d\theta$$

These equations are fully consistent with those found in Yoshida and Saito (2006) and Ziatdinov *et al.* (2012). Yoshida and Saito point out the bounds for s and θ in order to assure that curvature is real. These are shown in Table 1.

	s			θ	
	upper	lower		upper	lower
$\alpha < 0$	$-1/\lambda\alpha$	—	$\alpha < 1$	$-1/\lambda(\alpha - 1)$	—
$\alpha = 0$	—	—	$\alpha = 1$	—	—
$\alpha > 0$	—	$-1/\lambda\alpha$	$\alpha > 1$	—	$-1/\lambda(\alpha - 1)$

Table 1: The upper and lower bounds for s and θ .

We now demonstrate the analytical solution for the log-aesthetic curves in terms of the tangent angle. The following transformation of variables will cast the integral in a more familiar form, let

$$t = -\frac{i}{\lambda(\alpha - 1)} [\lambda(\alpha - 1)\theta + 1] \tag{12}$$

$$\theta = it - \frac{1}{\lambda(\alpha - 1)} \quad d\theta = i dt$$

The integral then becomes

$$z(\theta) = \int [i\lambda(\alpha - 1)t]^{a-1} e^{i\left(it - \frac{1}{\lambda(\alpha - 1)}\right)} i dt = i [i\lambda(\alpha - 1)]^{a-1} e^{\frac{i}{\lambda(\alpha - 1)}} \int t^{a-1} e^{-t} dt \tag{13}$$

The integral is recognized as the incomplete gamma function and the solution can be written as

$$z(\theta) = -i [i\lambda(\alpha - 1)]^{a-1} e^{-\frac{i}{\lambda(\alpha - 1)}} \Gamma \left(a, -\frac{i[\lambda(\alpha - 1)\theta + 1]}{\lambda(\alpha - 1)} \right) \Bigg|_{\theta_0}^{\theta} \tag{14}$$

We can find $z(s)$ similarly. Let $t = -i(\lambda\alpha s + 1)^{\frac{1}{a}} / \lambda(\alpha - 1)$; we then find

$$z(s) = -i [i\lambda(\alpha - 1)]^{a-1} e^{-\frac{i}{\lambda(\alpha - 1)}} \Gamma \left(a, -\frac{i(\lambda\alpha s + 1)^{\frac{1}{a}}}{\lambda(\alpha - 1)} \right) \Bigg|_{s_0}^s \tag{15}$$

Equations (14) and (15) are in every way identical. These are analytic solutions, but not in closed-form because the incomplete gamma function itself is an infinite series. We can further “simplify” the solutions for the special case where the parameter $a = \alpha/\alpha - 1$ is an integer, because in that case the incomplete gamma function becomes [Olver *et al.* (2010)],

$$\Gamma(a, t) = (a-1)! e^{-t} \sum_{k=0}^{a-1} \frac{t^k}{k!} \tag{16}$$

Figure 5 shows some typical results for the log-aesthetic curves, here shown for $a = \alpha = 2$ and various λ , $\lambda \in [0.01, 0.05, 0.1, 1.0]$. This figure compares the solutions by direct numerical integration of Eq. (11), full incomplete gamma function, Eq. (14), and the finite summation, Eq. (16). The results are indistinguishable at the scale of the figure.

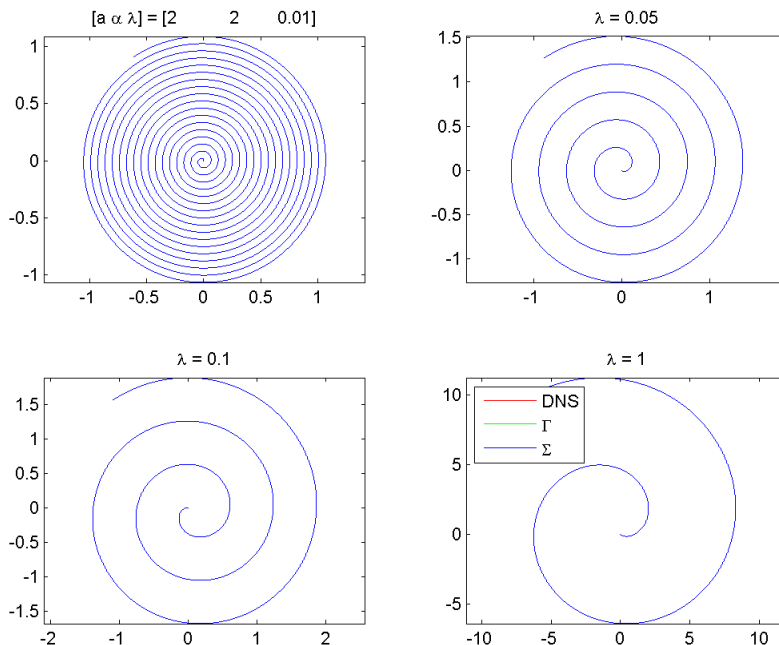


Figure 5: Log-aesthetic curves with $a = \alpha = 2$. (θ varies from its lower bound to 10 radians.)

We compared the computational efficacy of the three methods over a range of values for a and λ ; specifically, a -values in ascending powers of 2, i.e., $a \in [2, 4, 8, 16, 32, 64]$, and $\lambda \in [0.01, 0.05, 0.1, 1.0]$. The computation was performed with the integration limits shown in Table 1. For values of $a \gtrsim 75$ the incomplete gamma function and polynomial methods run into overflow problems, but the direct numerical simulation has no such problems (the largest value we tried was $a = 2^{12}$).

The aggregate time for the computation all 24 cases for each method, representing a broad range of a and λ values, are shown in Table 2. Calculations were performed with 10^5 and 10^6 θ -values. The calculations were carried out on Pentium 6-core i7 3.20 GHz computer using Matlab. The exceptional speed of the DNS can be attributed to the Matlab function `cumtrapz`; this is in lieu of 10^5 - 10^6 for loop calculations.

Time (s) to calculate all 24 cases		
Method	$\Delta\theta = \mathcal{O}(10^{-5})$	$\Delta\theta = \mathcal{O}(10^{-6})$
DNS: $\int_0^\psi \rho(\theta) e^{i\theta} d\theta$	0.23	3.25
IGF: $f(a, \lambda) \cdot \Gamma(a, t)$	12.3	128.6
Poly: $f(a, \lambda) \cdot e^{-t} \sum_{k=0}^{a-1} \frac{t^k}{k!}$	1.65	14.2

Table 2: Representative calculation times for various integration methods .

There is one *very* important cautionary note to be made here. We have been rather cavalier here in that we used a simple trapezoidal integration. The integrands in Eqs. (4), (5), and (11) are highly oscillatory and therefore require special attention. We dodged the bullet here by choosing an adequately small integration step size, but that might not always be possible. Figure 6 shows a detail from a re-calculation of the Euler polynomial spiral (Figure 3) with a 100-fold increase in the integration step size. All those extra spirals are numerical artifacts.

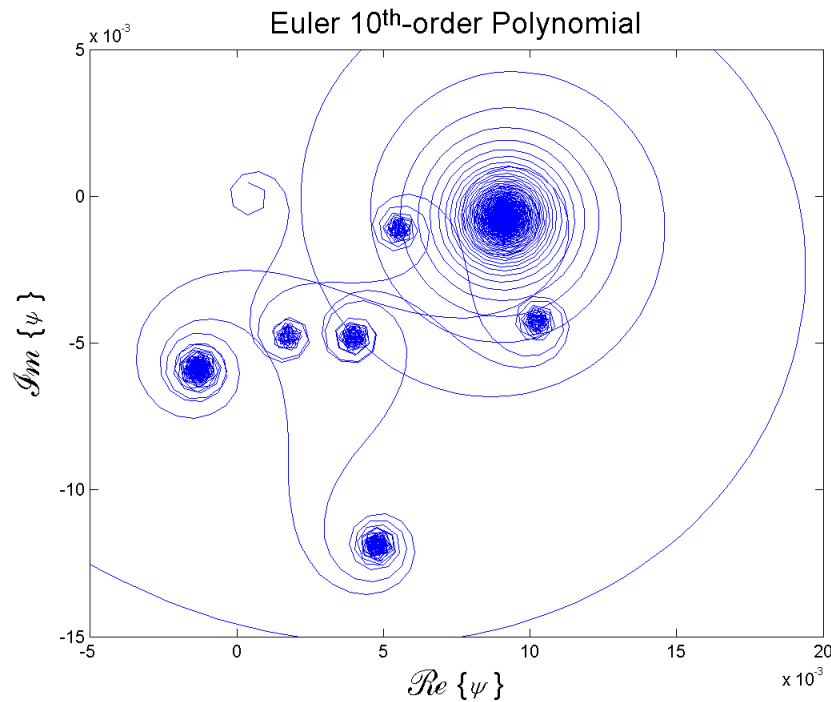


Figure 6: Detail of Figure 3 (upper right corner) with 100-fold increase in integration step size.

A new class of polynomial spirals?

The above analysis of the log-aesthetic curves suggests an alternative approach to polynomial spirals. The method will be outlined here and new analytic solutions derived. We begin with the tangent angle formulation of the curve, i.e.,

$$z(\theta) = \int \rho(\theta) e^{i\theta} d\theta \quad (17)$$

Now, we assume that the radius of curvature is a polynomial, say

$$\rho(\theta) = \sum_{j=0}^J a_j \theta^j \quad (18)$$

Substituting Eq. (18) into (17) and integrating, we obtain

$$z(\theta) = \sum_{j=0}^J a_j \int_{\theta_0}^{\theta} \theta^j e^{i\theta} d\theta = \sum_{j=0}^J -i^{j+1} a_j [\Gamma(j+1, -i\theta) - \Gamma(j+1, -i\theta_0)] \quad (19)$$

Or, invoking Eq. (16), we can eliminate the incomplete gamma function in favor of the finite summation, to wit,

$$z(\theta) = \sum_{j=0}^J -i^{j+1} a_j j! \left[e^{i\theta} \sum_{k=0}^j \frac{(-i\theta)^k}{k!} - e^{i\theta_0} \sum_{k=0}^j \frac{(-i\theta_0)^k}{k!} \right] \quad (20)$$

This is not very pretty, but it's effective. There are no special functions and the calculation is straightforward. We can relate the solution to the arc length as follows,

$$\begin{aligned} \frac{ds}{d\theta} &= \rho \\ s &= \int \rho d\theta = \sum_{j=0}^J \frac{a_j}{j+1} \theta^{j+1} \end{aligned} \quad (21)$$

These curves are ripe for exploration. All we have done so far is to verify that the solutions in Eqs. (17)-(20) are numerically equivalent. Figure 7 shows the results for a radius curvature defined by a random 6th-order polynomial for $\theta \in [0, 10\pi]$. (The curves have scaled down by a factor of 10^9). The calculation times for $\Sigma \Gamma : \Sigma \Sigma : \text{DNS} = 37.0 : 1.3 : 0.2$ seconds for Eqs. (19), (20), and (17), respectively, with 10^6 integration points. Mathematically, these solutions permit negative values of ρ ; the curves have cusps at those points. We will leave this for the reader to resolve.

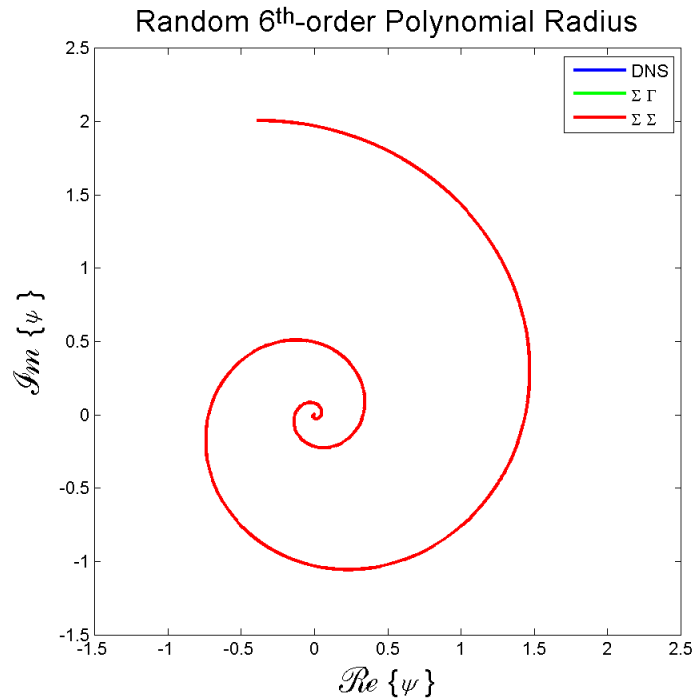


Figure 7: Curves for a random 6th-order polynomial radius of curvature for $\theta \in [0, 10\pi]$.

References

- Burchard, H.G. *et al.* (1994), “Approximation with Aesthetic Constraints ,” in *Designing Fair Curves and Surfaces: Shape Quality in Geometric Modeling and Computer-aided Design*, N.S. Sapidis, Ed., SIAM.
- Dillen, F. (1990), “The Classification of Hypersurfaces of a Euclidean Space with Parallel Higher Order Fundamental Form,” *Mathematische Zeitschrift* 203:635–643.
- Olver, F.W.J., Lozier, D.W., Boisvert, R.F., and Clark, C.W., (2010), *NIST Handbook of Mathematical Functions*. Cambridge University Press, New York.
- Yoshida, N. and Saito, T. (2006). “Interactive Aesthetic Curve Segments,” *The Visual Computer*, **22** (9), 896-905.
- Ziatdinov, R., Yoshida, N., and Kim, T, (2012). “Analytic parametric equations of log-aesthetic curves in terms of incomplete gamma functions,” *Computer Aided Geometric Design*, **29** (2), 129-140.
- Zwicker, C. (1963). *The Advanced Geometry of Plane Curves and Their Applications*, Dover Press.